Direct Presentation of a Melanocyte-Associated Antigen in Peripheral Lymph Nodes Induces Cytotoxic CD8(+) T Cells

Article *in* Cancer Research · November 2008

DOI: 10.1158/0008-5472.CAN-08-0809 · Source: PubMed

CITATIONS
11

READS
427

9 authors, including:

Emmanuel Contassot
University of Zurich
105 PUBLICATIONS **5,053** CITATIONS
SEE PROFILE

Magali Irla
Centre d'Immunologie de Marseille-Luminy
86 PUBLICATIONS **1,586** CITATIONS
SEE PROFILE

Stéphanie Hugues
University of Geneva
103 PUBLICATIONS **6,704** CITATIONS
SEE PROFILE

Olivier Preynat-Seauve
University of Geneva
66 PUBLICATIONS **1,639** CITATIONS
SEE PROFILE

Direct Presentation of a Melanocyte-Associated Antigen in Peripheral Lymph Nodes Induces Cytotoxic CD8$^+$ T Cells

Prisca Schuler,[1] Emmanuel Contassot,[1] Magali Irla,[2] Stéphanie Hugues,[2] Olivier Preynat-Seauve,[1] Friederich Beermann,[3] Alena Donda,[4] L.E. French,[1] and Bertrand Huard[1]

[1]Louis Jeantet Laboratory, Skin Cancers, Department of Dermatology and [2]Department of Pathology-Immunology, University Medical Center, Geneva, Switzerland and [3]Swiss Institute for Experimental Cancer Research; [4]Biochemistry institute, Lausanne University, Epalinges, Switzerland

Abstract

Encounter of self-antigens in the periphery by mature T cells induces tolerance in the steady-state. Hence, it is not understood why the same peripheral antigens are also promiscuously expressed in the thymus to mediate central tolerance. Here, we analyzed CD8$^+$ T-cell tolerance to such an antigen constituted by ovalbumin under the control of the tyrosinase promoter. As expected, endogenous CD8$^+$ T-cell responses were altered in the periphery of transgenic mice, resulting from promiscuous expression of the self-antigen in mature medullary epithelial cells and deletion of high-affinity T cells in the thymus. In adoptive T-cell transfer experiments, we observed constitutive presentation of the self-antigen in peripheral lymph nodes. Notably, this self-antigen presentation induced persisting cytotoxic cells from high-affinity CD8$^+$ T-cell precursors. Lymph node resident melanoblasts expressing tyrosinase directly presented the self-antigen to CD8$^+$ T cells, independently of bone marrow–derived antigen-presenting cells. This peripheral priming was independent of the subcellular localization of the self-antigen, indicating that this mechanism may apply to other melanocyte-associated antigens. Hence, central tolerance by promiscuous expression of peripheral antigens is a mandatory, rather than a superfluous, mechanism to counteract the peripheral priming, at least for self-antigens that can be directly presented in lymph nodes. The peripheral priming by lymph node melanoblasts identified here may constitute an advantage for immunotherapies based on adoptive T-cell transfer. [Cancer Res 2008;68(20):8410–8]

Introduction

Two pathways have been described mediating T-cell tolerance to self-antigens. These two pathways are very distinct because they act at different places and at different stages of T-cell maturation. The first one, called central tolerance, is achieved in the thymus with the presentation of self-antigens to maturating T cells via direct and cross-presentation by thymic epithelial cells and bone marrow–derived antigen-presenting cells (BM APC), respectively (1). The second one, called peripheral tolerance (2), is achieved outside the thymus on mature T cells with the presentation of self-antigens in secondary lymphoid organs via cross-presentation by BM APC (3). Combining the two pathways does not result in a perfect process. Indeed, both exhibit similar dysfunctions with less efficiency during early life (4, 5) and sparing of low-affinity T cells (6) so that pathogenic autoreactive T cells can be active in autoimmune diseases (7). Hence, the redundancy between central and peripheral tolerance is not understood, especially for the peripheral antigens that are promiscuously expressed in the thymus (8).

The skin may be a peculiar organ in terms of peripheral tolerance. Indeed, peripheral presentation of a self-antigen expressed in the skin induces cytotoxic CD8$^+$ T cells with pathogenic activity (9). This is the first organ described to date to induce such pathogenic T cells in the steady-state. In this case, a potent thymic deletion is needed to ensure tolerance (10). The antigen used in these models was expressed in keratinocytes. Another important component of the skin is the melanocyte. A partial T-cell tolerance has been reported for different melanocyte-associated antigens (MAA; ref. 11), including tyrosinase (12). However, it is not known whether this is due to a peripheral mechanism, a central mechanism, or both.

Here, we analyzed CD8$^+$ T-cell tolerance to MAA by using expression of a model self-antigen ovalbumin (OVA) under the control of regulatory elements from the tyrosinase promoter. We selected tyrosinase for two reasons. First, tyrosinase is promiscuously expressed in mouse (13) and human (14) thymus. Second, tyrosinase is a tumor rejection antigen (15, 16), rendering essential a better understanding of the tolerance mechanism(s) acting for this antigen to improve current melanoma immunotherapy.

Materials and Methods

Mice. A cytoplasmic form of ovalbumin (OVAcyt) was created by PCR-assisted deletion of the first 45 amino acids containing the OVA secreted signal sequence (17). The membrane-bound form (OVAmb) was created by PCR-assisted fusion of the 60 NH_2 terminal amino acids of the human OX40L, including signal peptide and transmembrane domain, with $OVA_{45\text{-}378}$. Insertion of the OX40L fragment created three alanines in the hinge region. These recombinant OVA DNA were cloned into pcDNA 3.1 (Invitrogen). Tyr-OVA mice were obtained by microinjection in fertilized oocytes from 129/Sv mice of the recombinant OVA cDNAs after subcloning into p(hs/-6.1)TyrCREBM1 vector (kindly provided by Ruth Ganss), containing the murine tyrosinase promoter (Tyr; ref. 18). Tyr-OVA mice were backcrossed at least six times on the C57BL/6 background (Tyr-OVA^{B6}). Some Tyr-OVA^{B6} mice were further backcrossed twice on the DBA/2 background to obtain Tyr-OVA mice homozygous for $H2^d$ (Tyr-$OVA^{DBA/2}$). For chimeric mice, recipient mice received 10×10^6 sex-matched bone marrow cells from donor mice in the lateral tail vein 20 h after total body irradiation (1,000 rad). Seven weeks after transplantation, H-2 phenotypes of grafted recipients were determined by immunostaining of peripheral blood

Note: Supplementary data for this article are available at Cancer Research Online (http://cancerres.aacrjournals.org/).

Current address for E. Contassot and L.E. French: Department of Dermatology, University Hospital, Zurich, Switzerland. Current address for B. Huard: Hematology Unit and Department of Pathoimmunology, Medical University Center, Geneva, Switzerland.

Requests for reprints: Bertrand Huard, Louis Jeantet Laboratory, University Medical Center, rue Michel Servet 1, 1211 Geneva 4, Switzerland. Phone: 41-22-379-58-11; Fax: 41-22-379-58-02; E-mail: bertrand.huard@medecine.unige.ch.

doi:10.1158/0008-5472.CAN-08-0809

cells with H-2^b and H-2^d specific monoclonal antibody (mAb). Reconstitution efficiency was >95% in all the chimeric mice used. OT-I mice express a transgenic T-cell receptor specific for the $OVA_{257-264}$ SIINFEKL peptide in the context of H-2K^b (kindly provided by W. Heath, WEHI Institute). OT-I × Tyr-OVA mice were obtained by crossing homozyguous OT-I mice with Tyr-OVA mice, and selection of animals bearing OVA DNA in the offsprings. OT-I T cells from *RAG-1*$^{-/-}$ mice kindly provided by Hans Acha-Orbea were used for transfer experiments in chimeric mice. Skin-draining lymph nodes (SDLN) from the melanocyte-deficient *kit*$^{W\text{-}sh}$ and *mitf*$^{mi\text{-}bw}$ mice were from the RIKEN Bioresource Center. *kit*$^{W\text{-}sh}$ mice were used as heterozygous due to infertility of the homozygous strain. All animal experiments were performed with groups of four to five mice under the agreement of the local veterinary office.

Reverse transcription–PCR studies. Total RNAs were extracted using TriZol according to manufacturer's protocol (Invitrogen) and treated with RQ1 DNase (Promega). Nonquantitative reverse transcription–PCR (RT-PCR) was performed as described (19) with 5′-CAGTGTGTGAAGGAACTG-3′ and 5′-TTCCTCCATCTCATGCG-3′ for OVA and 5′-ATATCGCTGCGCTGGTCGTC-3′ and 5′-AGGATGGCGTGAGGAGAGC-3′ for control β-actin. For real-time PCR, cDNA was synthesized from 1 μg of RNA using random hexamer primers and Superscript II reverse transcriptase (Invitrogen), and the following primers were used: 5′-TAAGGATGAAGACACACAAGCA-3′ and 5′-TGATGCCACTCTAAATAAACCA-3′ for OVA, 5′-TCAGCCCAGCATCCTTCTTC-3′ and 5′-TAGTGGTCCCTCAGGTGTTC-3′ for tyrosinase, and 5′-CCAGCAGGTGTTTGAGTCAG-3′ and 5′-CACTCCGGGCCTTGTTCTTC-3′ for autoimmune regulator (AIRE). PCR was performed using the iCycler iQ real-time PCR detection system (Bio-Rad) and iQ SYBR green supermix. cDNA amounts were calculated by comparison to a standard curve generated with serial dilutions of a reference cDNA. All PCRs were repeated at least thrice. Expression levels between samples were normalized using the average values of 18S rRNA with the following primers: 5′-CTTAGAGGGACAAGTGGCG-3′ and 5′-ACGCTGAGCCAGTCAGTGTA-3′.

Flow cytometry. Recombinant OVA cDNAs were cloned into pcDNA3.1 and transfected in 293-T cells with calcium phosphate precipitation, as previously described (20). OVA protein localization was studied by immunostaining with a polyclonal antibody against OVA (Sigma) and flow cytometry analysis, as previously described (21). For *ex vivo* murine cell phenotyping, anti-CD3ε (clone 145-2c11), anti-CD4 (clone RM4-5), anti-CD8 (clone 53-6.7), anti-CD11c (clone N418), anti-CD25 (clone PC61), anti-CD44 (clone IM7), anti-CD45 (clone 30F11), anti-CD62-L (clone Mel-14), anti-CD80 (clone 16-10A1), anti-Vα2 (clone B20.1), anti-Vβ5 (clone MR9-4), anti-H2-D^b (clone KH95), anti-H2-D^d (clone 34-2-12), anti-MHC class II (clone M5/114), and the corresponding isotype control antibodies were from BD PharMingen. P-selectin ligand expression was analyzed using P-selectin human Fc fusion protein (BD PharMingen), and secondary PE-conjugated goat anti-human IgG. H-2K^b/$OVA_{257-264}$ tetramers were prepared according to Kalergis and colleagues (22).

Immunohistochemistry. Mouse tissues were fixed in 4% buffered formalin for 24 h, paraffin-embedded, sectioned at 5-μm thickness, stained, and visualized as previously described (20). Stainings were performed with the pep-7 anti-tyrosinase, pep-8 anti–TRP-2, and pep-13 anti–gp100 rabbit sera, kindly provided by Vincent Hearing. These polyclonal sera made against the human sequences, all cross-reacted against the corresponding mouse proteins. They were all used at 1/400. The mouse mAb against TRP-1, Mel-5 (5 μg/mL) was from Signet Laboratories. Detection antibodies were goat immunoglobulin anti-rabbit or anti-mouse IgG conjugated to biotin (Jackson Immunoresearch), and revelation was performed with StreptABComplex/horseradish peroxidase (HRP; Dako). For detection of OVA protein, a home-made mouse polyclonal serum was generated against OVA and revelation was performed with an enhanced system ("envision"^{plus} HRP, Dako).

Purification of thymic cells. Twenty thymi were pooled for cell purification. Six Tyr-OVAcyt, six Tyr-OVAsec, and eight Tyr-OVAmb mice, as well as 20 age-matched and sex-matched C57BL/6, were used. Thymic cellular suspension was incubated with the anti-FcR mAb 2.4G2 (BD PharMingen) for 15 min at 4°C and sorted into CD45$^+$ and CD45$^-$ populations using anti-CD45 microbeads and Automacs (Miltenyi Biotech). CD11c$^+$MHC class II$^+$ dendritic cell (DC) and CD11c$^-$ MHC class II$^+$ macrophages/B cells were purified from the CD45$^+$ population. Mature and immature mTEC, defined as MHC class II$^+$, expressing a high level of CD80 and MHC class II$^-$ CD80$^-$, respectively, were sorted from the CD45$^-$ population with a FACS-ARIA (BD Biosciences).

Immunization and B16-OVA challenge. For DNA vaccination, groups of five mice were immunized twice at 2 wk apart in inguinal lymph node (23) with 10 μg of the pNDK-OVA plasmid encoding the full-length OVA, kindly provided by M. Bevan. For peptide immunization, mice were challenged s.c. with 20 μg of the SIINFEKL peptide corresponding to $OVA_{257-264}$, synthesized according to the F-moc strategy at the Biochemistry Institute of Lausanne and emulsified in complete Freund adjuvant (CFA; Sigma). DCs were generated from mouse bone marrow precursors in the presence of granulocyte macrophage colony-stimulating factor/interleukin-4, as previously described (24). After 5 d of culture, they were loaded with 2 mg/mL of OVA for 4 h at 37°C and washed twice in PBS and 1 × 10^6 cells were injected s.c. twice a week apart. Plasmid encoding the cytoplasmic form of OVA was electroporated in the melanoma cell line

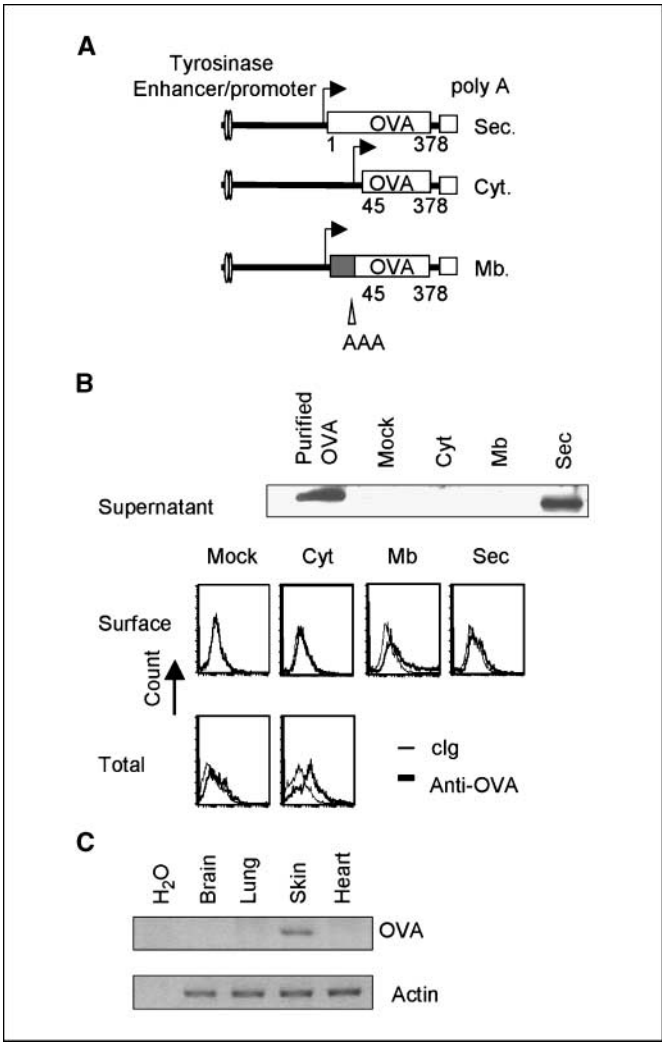

Figure 1. Generation of Tyr-OVA mice expressing secreted, cytoplasmic, or membrane OVA in the skin. C57BL/6 mice expressing three different forms of OVA in melanocytes were generated by transgenesis of OVA cDNAs under the control of the tyrosinase promoter. *A,* scheme of the Tyr-OVA transgenes created with different subcellular localizations. *B,* OVA localization was studied in supernatants from transiently transfected 293-T cells by Western blot (*top*). Purified OVA (10 ng) was used as standard. OVA localization was also studied by flow cytometry at the surface of viable (*middle*) or in permeabilized (*bottom*) 293-T–transfected cells. *C,* RT-PCR analysis of OVA and control actin mRNA expression in the indicated organs from Tyr-OVA mice.

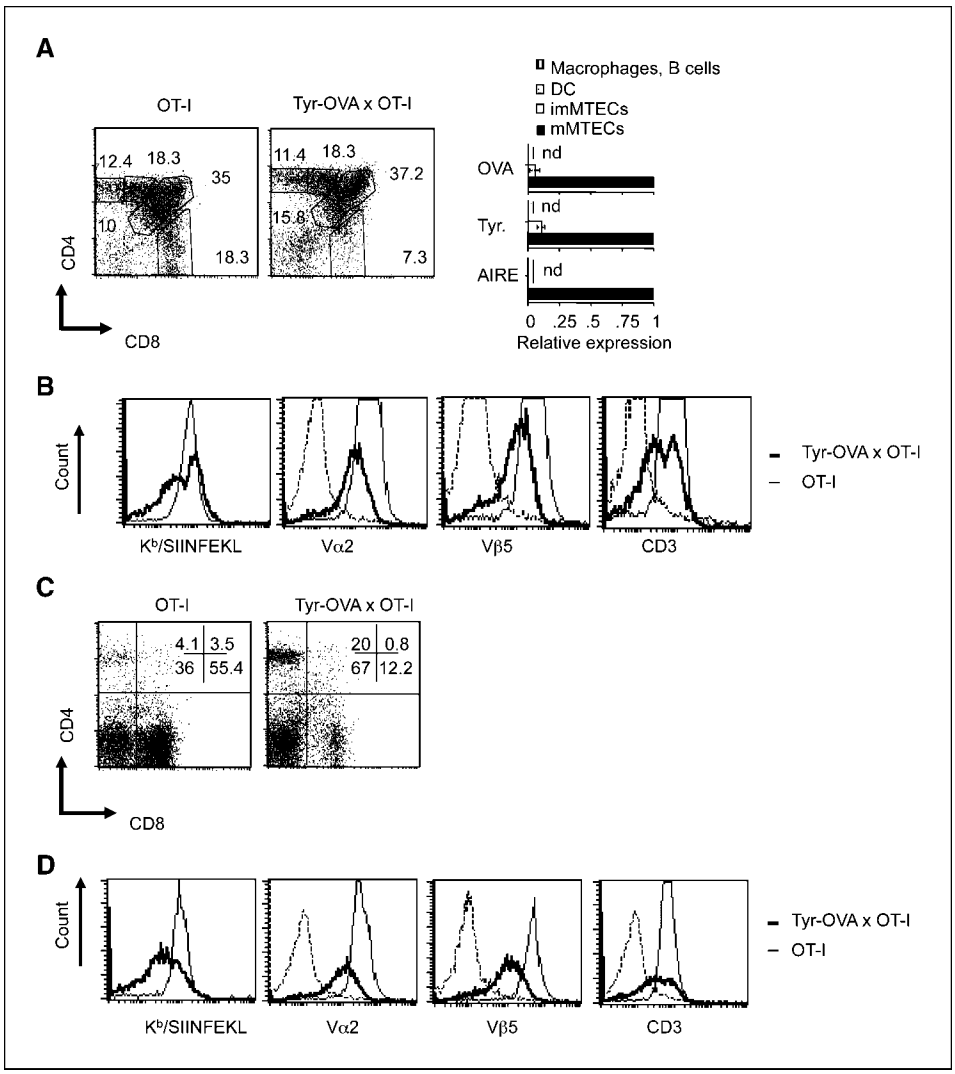

Figure 2. Central deletion of OT-I T cells in Tyr-OVA × OT-I mice. *A,* CD8/CD4 T-cell subsets were studied in thymi of OT-I and Tyr-OVAcyt × OT-I mice (*left*). Percentages obtained for the different thymocyte subsets are indicated. mRNA expression was analyzed by quantitative RT-PCR for OVA, tyrosinase, and AIRE expression in the indicated cells (*right*). *nd,* not detected. *B,* levels of Vα2, Vβ5, and CD3 expressions and K^b/SIINFEKL tetramer binding are shown for representative mice on gated single-positive $CD8^+$ thymocytes. *Dotted lines,* isotype control. *C,* CD8/CD4 T-cell subsets were studied in SDLN (axillary and inguinal). *D,* immunostaining for Vα2, Vβ5, and CD3 expressions and K^b/SIINFEKL tetramer binding in SDLN on gated $CD8^+$ T cells. Similar data were obtained with double transgenic Tyr-OVAsec × OT-I and Tyr-OVAmb × OT-I mice.

B16F10, kindly provided by I. Fidler. Transfected B16F10 cells were selected with 1 mg/mL of G418 (Invitrogen) and cloned twice by limiting dilution. 5×10^4 B16-OVA cells were injected s.c. 1 to 2 wk after the last boost. Tumor growth was monitored every other day. Mice were sacrificed when tumor surface reached 1 cm^2.

***In vivo* OT-I T-cell proliferation and cytotoxicity.** *In vivo* OT-I T-cell proliferation was assessed as previously described (24). For transfer in chimeric mice, OT-I $CD8^+$ T cells were negatively selected with the mouse CD8 selection kit and an automacs (Miltenyi). 2×10^6 purified cells were injected in this case. *In vivo* cytotoxicity was assessed 8 d after transfer of unlabeled OT-I T cells. For this assay, C57BL/6 splenocytes were labeled with either 2.5 (high) or 0.25 (low) μmol/L CFSE and pulsed with 1 μmol/L of SIINFEKL peptide or irrelevant H-$2K^b$ restricted gp33 peptide, respectively. After 90 min at 37°C, cells were washed and equal numbers of both populations were mixed and transferred i.v. After 18 h, $CFSE^+$ cells were numerated by flow cytometry and the percentage of specific cytotoxicity was calculated.

Statistics. All data in graphs and plots are presented as mean ± SD. Statistical analysis in Fig. 3*B* used a log-rank test. Statistical analysis in Fig. 6*C* used a Mann-Whitney test with a two-tail *P* value.

Results

Generation of Tyr-OVA mice. We used OVA as a model self-antigen. To modulate the subcellular localization of the self-antigen, we generated recombinant DNA encoding for cytoplasmic (cyt) and transmembrane (mb) OVA, in addition to the natural secreted (sec) OVA (Fig. 1*A*). We first tested these three DNA for expression in transiently transfected 293-T cells. Figure 1*B* shows that only the secreted form was present in cell supernatants (*top*). In contrast, OVAmb was the unique form present at the cell surface on a significant fraction of transfected cells (*middle*), whereas we detected OVAcyt in transfected cells only after cell permeabilization (*bottom*). Altogether, this analysis shows that the three different forms of OVA generated were expressed at the correct subcellular localization. The three OVA cDNAs were then placed under regulatory elements of the melanocyte-specific tyrosinase promoter known to recapitulate endogenous tyrosinase expression (18). We generated transgenic mice and selected lines expressing 20%, 3%, and 20% OVA mRNA in the skin compared with endogenous tyrosinase for OVAsec, OVAcyt, and OVAmb, respectively. We detected no expression of OVA mRNA in control organs, such as brain, heart, and lung (Fig. 1*C*).

Thymic deletion of self-antigen–specific $CD8^+$ T cells in Tyr-OVA mice. We crossed Tyr-OVA mice with OT-I mice and first investigated $CD8^+$ T-cell tolerance in these double transgenic animals. We used OT-I mice on a RAG-sufficient background to allow potential endogenous gene rearrangement. We observed a

2.5-fold to 4-fold reduction in the number of single-positive $CD8^+$ thymocytes in the chest thymus compared with single transgenic OT-I mice (Fig. 2*A, left*). $CD4^+CD8^-$ and $CD4^-CD8^-$ thymocytes slightly increased. As a consequence, the overall thymic cellularity did not significantly change (data not shown). We also observed deletion of single-positive $CD8^+$ thymocytes in the cervical thymus (data not shown) identified as a second functional mouse thymus (25). Promiscuous expression of transgenic OVA in the thymus explained this central deletion. Indeed, quantitative RT-PCR showed OVA mRNA in the thymus similar to endogenous tyrosinase, with predominance in $CD45^-CD80^{high}$ MHC class II^{high} mature medullary thymic epithelial cells (MTEC), expressing the transcription factor AIRE (Fig. 2*A, right*). Immature MTEC expressed weakly OVA and thymic DC, and macrophages were negative. On the remaining single-positive $CD8^+$ thymocytes, almost half of the cells had a decreased binding of H2-K^b/SIINFEKL tetramer (Fig. 2*B*). This decreased binding correlated with a down-regulation of Vα2, Vβ5, and CD3, indicating that the diminished tetramer binding was the consequence of a TCR/CD3 down-regulation. This TCR/CD3 down-regulation was already evident on $CD4^+CD8^+$ thymocytes (data not shown) and was likely engaged on a fraction of $CD4^+CD8^+$ thymocytes to escape negative selection.

We observed similar alterations of the $CD8^+$ T-cell repertoire in SDLNs of Tyr-OVA × OT-I mice. Indeed, $CD8^+$ T cells decreased to a similar extent (Fig. 2*C*), and TCR/CD3 was down-regulated from the surface of a similar fraction of peripheral cells (Fig. 2*D*). Meanwhile, the number of peripheral $CD4^+$ T cells increased. The presence of these latter cells is not specific to our transgenic model because they are present in K14-OVA transgenic mice (10). These cells expressed the transgenic Vα2/Vβ5 TCR but did not bind H2-K^b/SIINFEKL tetramer, most likely because of their lack of CD8 expression (Supplementary Fig. S1; ref. 26). In addition, they did not express CD25, differentiating them from natural regulatory T cells. The immune relevance of these cells warrants further investigations. We also observed OT-I T-cell reduction and phenotype alteration in lymphoid organs distant from the skin, such as mesenteric lymph nodes (data not shown), indicative of a systemic phenotype.

The presence of mature OT-I T cells in the periphery indicates that central tolerance was either not complete or was submerged by the artificially high number of TCR-transgenic T cells. To discriminate between the two, we next studied $CD8^+$ T-cell tolerance for an endogenous repertoire. We vaccinated Tyr-OVA mice with OVA DNA and challenged them later on with a lethal dose of B16-OVA. As expected, OVA DNA vaccination resulted in

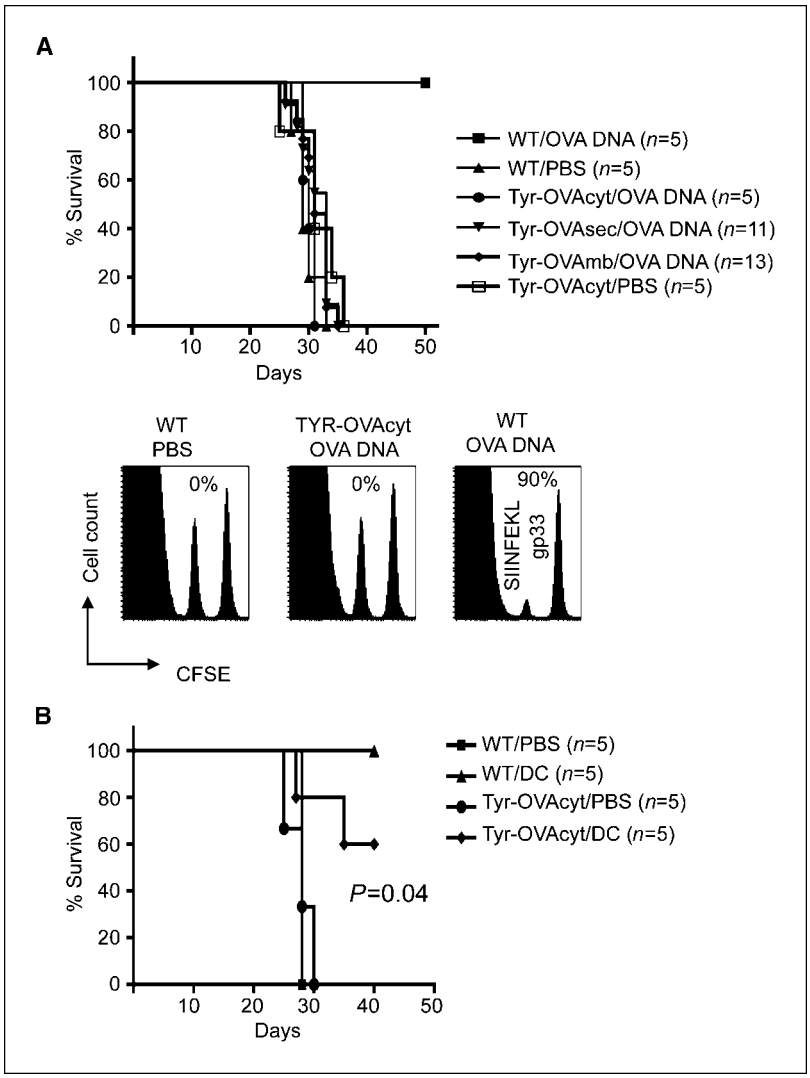

Figure 3. Deficient generation of anti-OVA CTL in Tyr-OVA mice upon DNA vaccination. *A,* WT or Tyr-OVAcyt, Tyr-OVAsec, Tyr-OVAmb mice were vaccinated with OVA DNA or PBS and challenged with a lethal dose of B16-OVAcyt. Survival is shown over a period of 50 d (*top*). *In vivo* cytotoxicity was performed in WT or Tyr-OVAcyt mice vaccinated with OVA DNA. CFA/SIINFEKL challenge in WT mice was used as positive control. Histogram plots show the remaining target cell populations in SDLN. Similar results were obtained in a repeat experiment with Tyr-OVAmb and Tyr-OVAsec mice (*bottom*). *B,* WT or Tyr-OVAcyt mice were vaccinated with OVA-loaded DC or PBS and challenged with a lethal dose of B16-OVAcyt. Survival is shown as in *A*.

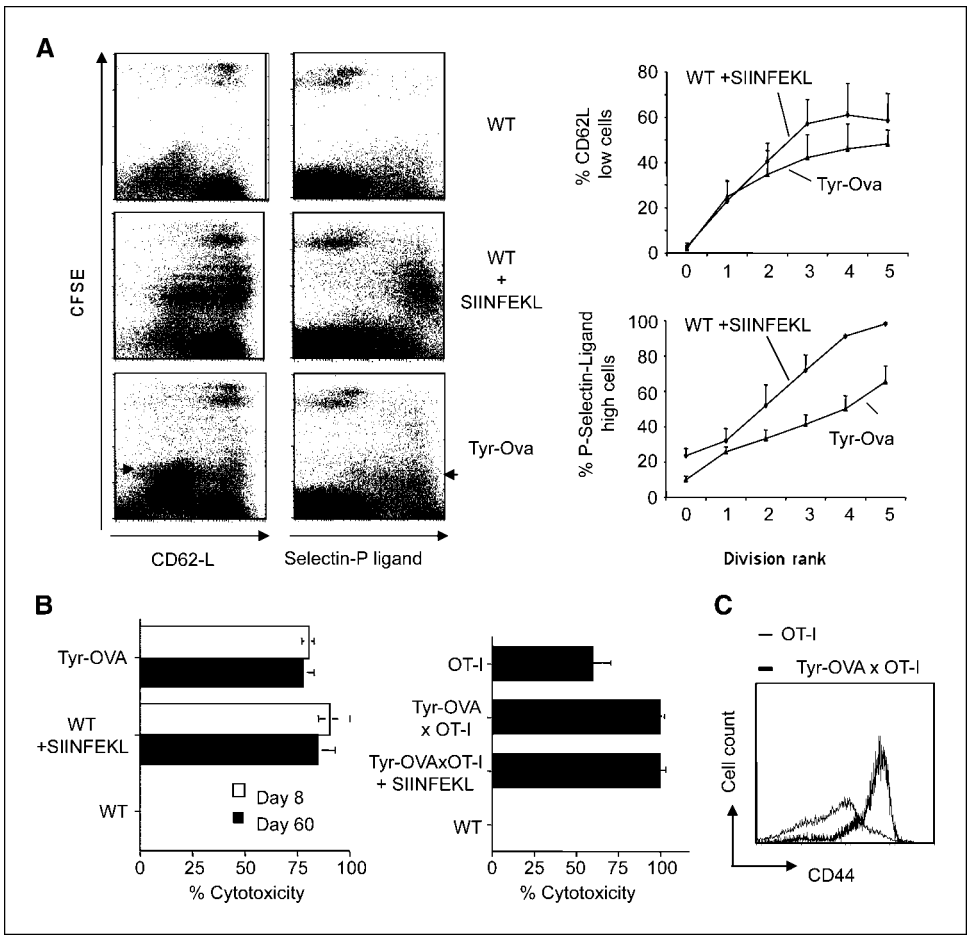

Figure 4. Presentation of OVA induces persisting cytotoxic OT-I T cells in the periphery of Tyr-OVA mice. *A,* CFSE-labeled OT-I T cells were transferred in WT or Tyr-OVAcyt mice. Dot plots show CFSE and CD62-L or P-selectin ligand stainings in SDLN (*left*). Percentages ± SD of cells with a down-regulated CD62-L and an up-regulated P-selectin ligand expression is shown from the indicated division rank (*right*). *B, in vivo* SIINFEKL-specific cytotoxicity was studied in SDLN from Tyr-OVA mice 8 and 60 d after transfer with OT-I T cells (*left*) or from untransferred Tyr-OVA × OT-I mice (*right*). The mean cytotoxicity ± SD obtained is indicated. Transfer experiments were performed in Tyr-OVAcyt and Tyr-OVAsec. *C,* level of CD44 expression on OT-I T cells in SDLN of OT-I compared with Tyr-OVAcyt × OT-I mice.

complete protection of C57BL/6 wild-type (WT) mice (Fig. 3*A, top*). However, 100% tyr-OVA mice died from tumor outgrowth, with no improvement in the survival compared with mock-vaccinated Tyr-OVA mice, indicating that OVA DNA vaccination was ineffective in these mice. The absence of protection in Tyr-OVA mice was due to deficient $CD8^+$ T-cell functions, because we observed no detectable CTL specific for SIINFEKL in vaccinated Tyr-OVA mice (Fig. 3*A, bottom*). In fact, only DC vaccination constituting a stronger vaccination regimen than naked DNA gave a significant protection against B16-OVA in Tyr-OVA mice (Fig. 3*B*). Together, these experiments show that $CD8^+$ T cells specific for the immunodominant SIINFEKL epitope are strongly altered in Tyr-OVA mice and that only a strong vaccination regimen with antigen-loaded DC generates tumoricidal T cells from this altered repertoire.

Constitutive self-antigen presentation induces cytotoxic $CD8^+$ T cells in the periphery of Tyr-OVA mice. We next performed adoptive transfers of CFSE-labeled naive OT-I T cells to study peripheral tolerance. OT-I T cells responded to OVA presentation in SDLN of Tyr-OVA mice by proliferating extensively even more than after a CFA/SIINFEKL challenge in WT mice. Indeed, many responding T cells had almost lost their CFSE dye 3 days after transfer in Tyr-OVA mice (Fig. 4*A, arrowhead, left*). In the meantime, dividing cells changed expression of homing markers by down-regulating CD62-L and up-regulating P-selectin ligand (Fig. 4*A*). In addition to acquiring homing markers to egress lymph nodes, responding OT-I T cells also acquired effector function, since we observed killing of SIINFEKL-pulsed target cells in SDLN from Tyr-OVA mice transferred with OT-I T cells (Fig. 4*B, left*). We obtained this complete killing with transfer of a limited number (5×10^4) of purified OT-I T cells. Killing lasted up to 60 days after transfer, indicating that the cytotoxic cells generated persisted in the host. We also assessed functionality of the remaining OT-I T cells in the periphery of Tyr-OVA × OT-I mice. We observed a 100% *in vivo* SIINFEKL-specific cytotoxicity in SDLN upon vaccination with CFA/SIINFEKL in double transgenic mice (Fig. 4*B, right*). Remarkably, an *in vivo* SIINFEKL-specific cytotoxicity was present in double transgenic mice in the absence of vaccination. The latter cytotoxicity was over the one obtained in unvaccinated single transgenic OT-I mice, containing 4-fold more SIINFEKL-specific T cells (see Fig. 2*C*). Together, this indicates that the strong cytotoxicity obtained in unvaccinated Tyr-OVA × OT-I mice was not only due to the high frequency of SIINFEKL-specific T cells but also to the priming of OT-I T cells in the periphery. The latter is consistent with the CD44 up-regulation observed on most of the peripheral OT-I T cells in the periphery of Tyr-OVA × OT-I mice (Fig. 4*C*). Taken together, the presence of persisting cytotoxic T cells in lymph nodes shows that constitutive presentation of OVA is a priming event in the periphery of Tyr-OVA mice.

Self-antigen presentation in peripheral lymph nodes by nonhematopoietic cells induces cytotoxic $CD8^+$ T cells. To investigate the cells involved in the presentation process, we repeated transfer experiments in chimeric mice. Remarkably, we also observed OT-I T-cell division in Tyr-OVA mice reconstituted with bone marrow cells from DBA/2 mice, unable to present the

SIINFEKL peptide to OT-I T cells (Fig. 5*A, top*), indicating that radio-resistant cells were implicated in the presentation process. We saw this proliferation in SDLN, but also in mesenteric lymph nodes (MesLN; Fig. 5*A, middle*), excluding the involvement of skin Langerhans cells, which are also radioresistant (27), but unable to migrate to skin nondraining lymph nodes (28). Quantitatively, the proliferation induced by the radio-resistant cells was similar to the one obtained with cross-presenting hematopoietic cells in Tyr-OVA mice back-crossed on a DBA/2 background and reconstituted with a marrow from C57BL/6 mice (Fig. 5*A, bottom*). However, the quality of the response differed. OVA cross-presentation by hematopoietic cells alone resulted in the absence of cytotoxic T-cell generation, whereas presentation by nonhematopoietic cells alone induced potent OVA-specific cytotoxic $CD8^+$ T cells (Fig. 5*B*). When hematopoietic and nonhemapoietic cells coacted in unmanipulated Tyr-OVA C57BL/6 mice, we observed induction of cytotoxic $CD8^+$ T cells (see Fig. 4*B*).

Melanoblasts present directly the self-antigen to $CD8^+$ T cells in peripheral lymph nodes. Because the above experiments in chimeric mice strongly suggested a direct presentation process by a nonhematopoietic cell, we looked for cells expressing the self-antigen in peripheral lymph nodes. RT-PCR analysis indicated OVA expression in lymph nodes (SDLN and MesLN) from Tyr-OVA mice, similar to endogenous tyrosinase (Fig. 6*A, left*). Quantitative RT-PCR showed that OVA and tyrosinase mRNA expression in SDLN were 4 and 10 times less elevated than in the skin, respectively (Fig. 6*A, right*). There was no detection of OVA and tyrosinase in control lungs. With an enhanced revelation system, we observed a significant expression of OVA protein in lymph node cells by immunohistochemistry (Supplementary Fig. S2*A*). Notably, cells positive for tyrosinase with a similar morphology were present at a similar place in the lymph node. These cells expressed endogenous tyrosinase and other melanocyte-specific enzymes involved in melanin synthesis, such as Trp-1, Trp-2, and gp100 (Supplementary Fig. S2*B*), but were not pigmented as assessed by Fontana/Masson staining (data not shown). Tyrosinase-expressing cells were present in the nodal sinus and in larger numbers in the nodal capsule (Fig. 6*B*). They exhibited a large cytoplasm and no dendrites, a morphology more closely reminiscent to that of unpigmented nondendritic skin melanoblasts present in hair follicles of neonate mice (29) than that of pigmented dendritic adult skin melanocytes. We further observed that their number in SDLN was significantly reduced in mice deficient for melanocyte generation, such as mice bearing the inactivating mutations *bw* in the *mitf* (*microtpthalmia transcription factor*; ref. 30) and *W-sh* in the *c-kit* (31) loci (Fig. 6*C*). We also observed tyrosinase-expressing cells in MesLN (data not shown) and human lymph nodes (Supplementary Fig. S3). Taken together, these experiments indicate that nonhematopoietic cells directly present OVA to OT-I T cells within secondary lymphoid organs and that these cells belong to the melanocyte lineage.

Discussion

In the present study, we show that high-affinity T cells specific for OVA, such as the OT-I T cells used here, were centrally deleted in transgenic mice expressing OVA under the control of the tyrosinase promoter. In Tyr-OVA transgenic mice, OVA expression mirrored that of endogenous tyrosinase with a predominant expression in mature MTEC, as previously described (13). Such expression in MTEC likely results in the direct presentation of the self-antigen at the surface of these cells, mediating T-cell deletion (8). Alternatively, we do not exclude that central deletion may be induced by cross-presentation of the self-antigen by thymic DC (1). In the Tyr-OVA model, the subcellular localization of the self-antigen did not affect central deletion since we observed deletion to a similar extent for a secreted, transmembrane and intracytoplasmic localization of the antigen. Hence, central deletion may well apply for other MAA.

We did not observe, upon transfer of OT-I in Tyr-OVA mice, evidence for a partial T-cell activation and functional deletion, characterizing conventional peripheral tolerance pathways reported in other transgenic systems (32–34). Again, this absence of peripheral tolerance was independent of the subcellular localization of the self-antigen. Instead, OVA presentation in the periphery was associated with OT-I T-cell proliferation, expression of homing markers implicated in lymph node egress, and gain of

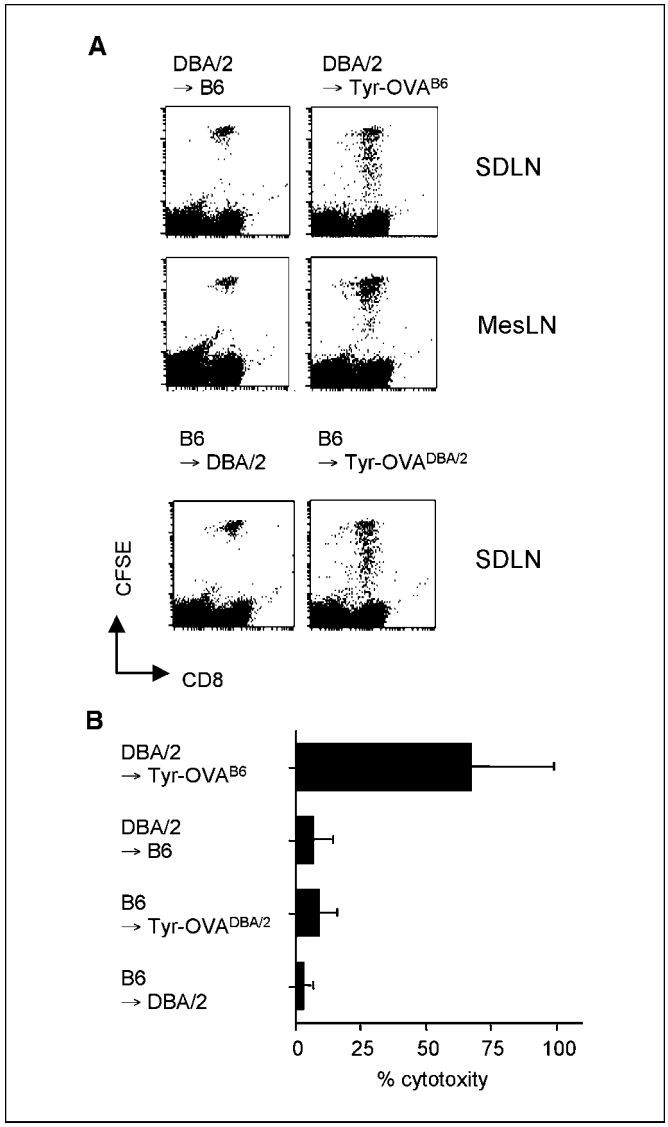

Figure 5. Radioresistant cells constitutively present OVA to $CD8^+$ T cells in the periphery of Tyr-OVA mice. *A,* CFSE-labeled OT-I T cells were transferred in the indicated chimeric mice. Dot plots show CFSE and CD8 staining 3 d after transfer in SDLN and MesLN. *B, in vivo* SIINFEKL-specific cytotoxicity was studied in SDLN and MesLN from the indicated chimeric mice 8 d after transfer with OT-I T cells. Mean cytotoxicity ± SD from groups of five mice is shown.

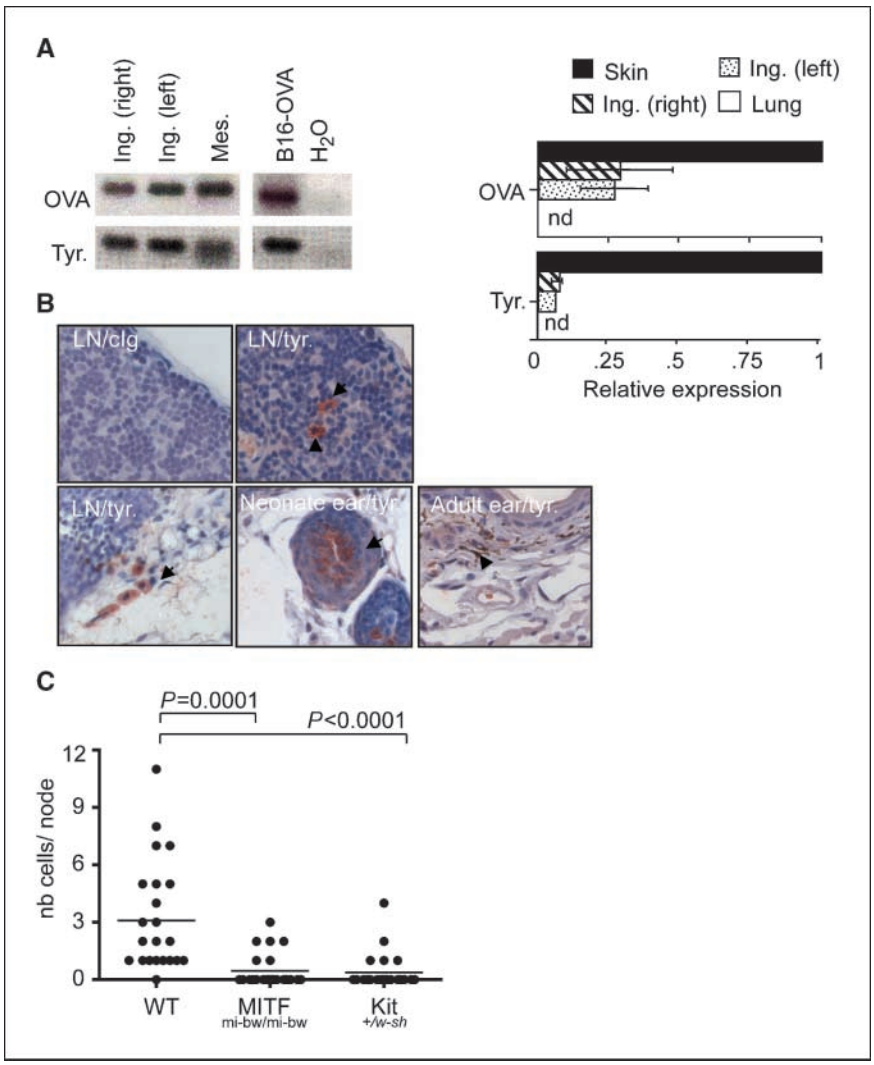

Figure 6. Presence of OVA-expressing melanoblasts in lymph nodes of Tyr-OVA mice. *A,* RT-PCR analysis of OVA and tyrosinase mRNA expression in SDLN and MesLN from Tyr-OVAcyt mice (*left*). Results are representative of three mice. Similar results were obtained in Tyr-OVAsec and Tyr-OVAmb mice. B16-OVA cells served as positive control. Quantitative RT-PCR analysis was performed for OVA and tyrosinase mRNA in the indicated organs from Tyr-OVAcyt mice (*right*). A value of 1 was arbitrarily given to gene expression in skin. *B,* the indicated organs from C57BL/6 mice were stained with a control immunoglobulin or an antityrosinase serum. Tyrosinase-stained cells are arrowed. Original magnification, 20×. *C,* the two inguinal and axillary lymph nodes from WT C57BL/6, *mitf*^{bw}, and *kit* $^{w\text{-}sh}$ were stained with the antityrosinase serum. Three mice per group were used, and lymph nodes were cut and stained twice. The number of tyrosinase-expressing cells counted per lymph node section is shown.

cytotoxic functions. Such peripheral priming of T cells by self-antigens is unexpected in a steady-state situation. Priming has already been observed by self-antigens expressed in other organs, such as pancreas, liver, lung, and intestine, but this occurred when high number of specific cells was present, artificially converting a nonpriming event into a priming one (35). Here, we observed peripheral priming upon transfer of a low number of specific cells shown to be insufficient to produce cytotoxic cells for a nonpriming event (36). Despite an efficient priming of OT-I T cells occurring in SDLN, no vitiligo-like skin lesion was observed in Tyr-OVA mice. This absence of pathologic autoimmunity warrants further investigations but is most likely due to the lack of concomitant skin inflammation and/or the lack of $CD4^+$ T-cell help required in similar skin experimental systems (37, 38). Nevertheless, the presence of cytotoxic cells may represent a danger for an organism, explaining the requirement of central tolerance for such antigens to minimize autoimmunity susceptibility.

Others also reported peripheral presentation of MAA in skin-distant mesenteric lymph nodes for an antigen controlled by the tyrosinase-related protein-2 promoter (39) and, recently, for tyrosinase itself (40). One attractive candidate as antigen-presenting cell in the presentation process is the melanocyte (or a melanocyte-like cell). Indeed, we detected mRNA and protein expression for OVA in lymphoid organs from Tyr-OVA mice, but also for endogenous tyrosinase, consistent with earlier work (41). Early data suspected the presence of melanocytes in lymphoid organs. This started by the clinical observation of melanoma developing in lymph nodes in the absence of primary cutaneous tumor, a pathology called blue nodal nevus (42). In this situation, the melanoma is postulated to originate from a melanocyte, arrested in lymphoid organs during its differentiation program. Another clinical observation is the occurrence of benign nodal nevi in lymph nodes draining primary melanoma (43). In this latter case, authors postulated an induction of proliferation for resident melanocytes selectively in nodes draining the primary cutaneous melanoma. Immunohistochemistry with specific antibodies allowed us to observe nodal cells expressing OVA and the endogenous tyrosinase protein, as well as other melanocyte-specific proteins, such as Trp-1, Trp-2, and gp100 in lymph nodes. Despite expression of all these enzymes involved in melanin synthesis, these cells were not pigmented, indicating that they may be more closely related to melanoblasts than fully differentiated melanocytes. The melanocytic origin of these cells was confirmed with the use of mutant mice. Mutations in the *kit* and *mitf* loci, known to impair melanocyte development, significantly reduced the number of tyrosinase-expressing cells in SDLN.

Immunohistochemistry also allowed us to locate these melanoblasts. Their position in the subcapsular zone of the lymph node is compatible with the development site of blue and nodal nevi and is consistent with a site associated to an efficient priming for $CD8^+$ T cells (44). Finally, their higher numbers in the capsule than in the sinus indicate that they may immigrate via the afferent lymph.

Tumor cells prime $CD8^+$ T cells in lymphoid organs despite tolerizing them when growing extralymphatically (45, 46). Here, we show that such priming also occurs for a self-antigen expressed by a nonprofessional antigen-presenting cell in the steady-state. The lymph node–resident melanoblasts identified in the present study are likely to be different from the stromal cells with a gene expression pattern resembling that of MTEC and mediating peripheral tolerance to intestinal self-antigens (47). Indeed, melanoblasts are too few compared with the cells stained with the mTEC-specific lectin *Ulex europaeus* agglutin-1 shown by Lee and colleagues and their localization was not restricted to the cortex. By contrast, these lymph node melanoblasts are likely to induce the peripheral deletion observed by Nichols and colleagues for $CD8^+$ T cells exhibiting an affinity sufficiently low to escape central tolerance (40). In contrast, they prime high-affinity $CD8^+$ T cells.

The contribution of this newly identified peripheral priming by lymph node melanoblast to melanoma immunotherapy is unclear. On one hand, this peripheral priming results overall in the elimination of all high-affinity T cells from the repertoire because it renders central tolerance mandatory. On the other hand, it may serve melanoma immunotherapy. Indeed, adoptive T-cell transfer (ACT) is believed to be the regimen of choice for tumor immunotherapy (48), and lymph node melanoblasts in this situation may provide the *in vivo* antigenic stimulus, recently identified as crucial for ACT efficacy (49). Tumor protection experiments after ACT in Tyr-OVA mice should help unravel whether lymph node melanoblasts may be helpful for melanoma immunotherapy.

Disclosure of Potential Conflicts of Interest

No potential conflicts of interest were disclosed.

Acknowledgments

Received 3/4/2008; revised 6/25/2008; accepted 7/25/2008.

Grant support: Louis Jeantet Foundation, Oncosuisse, and Association International for Cancer Research.

The costs of publication of this article were defrayed in part by the payment of page charges. This article must therefore be hereby marked *advertisement* in accordance with 18 U.S.C. Section 1734 solely to indicate this fact.

We thank S. Izui, C. Hauser, and G. Hollander for critical reading of the manuscript and Kerstin Grosdemange for technical expertise.

References

1. Gallegos AM, Bevan MJ. Central tolerance to tissue-specific antigens mediated by direct and indirect antigen presentation. J Exp Med 2004;200:1039–49.
2. Redmond WL, Sherman LA. Peripheral tolerance of CD8 T lymphocytes. Immunity 2005;22:275–84.
3. Heath WR, Kurts C, Miller JF, Carbone FR. Cross-tolerance: a pathway for inducing tolerance to peripheral tissue antigens. J Exp Med 1998;187:1549–53.
4. Gallegos AM, Bevan MJ. Central tolerance: good but imperfect. Immunol Rev 2006;209:290–6.
5. Mintern JD, Sutherland RM, Lew AM, Shortman K, Carbone FR, Heath WR. Constitutive, but not inflammatory, cross-presentation is disabled in the pancreas of young mice. Eur J Immunol 2002;32:1044–51.
6. Zehn D, Bevan MJ. T cells with low avidity for a tissue-restricted antigen routinely evade central and peripheral tolerance and cause autoimmunity. Immunity 2006;25:261–70.
7. Walter U, Santamaria P. CD8+ T cells in autoimmunity. Curr Opin Immunol 2005;17:624–31.
8. Anderson MS, Venanzi ES, Klein L, et al. Projection of an immunological self shadow within the thymus by the aire protein. Science 2002;298:1395–401.
9. Mayerova D, Parke EA, Bursch LS, Odumade OA, Hogquist KA. Langerhans cells activate naive self-antigen-specific CD8 T cells in the steady state. Immunity 2004;21:391–400.
10. McGargill MA, Derbinski JM, Hogquist KA. Receptor editing in developing T cells. Nat Immunol 2000;1:336–41.
11. Touloukian CE, Leitner WW, Schnur RE, et al. Normal tissue depresses while tumor tissue enhances human T cell responses *in vivo* to a novel self/tumor melanoma antigen, OA1. J Immunol 2003;170:1579–85.
12. Colella TA, Thompson L, Graham DD, et al. Self-tolerance to the murine homologue of a tyrosinase-derived melanoma antigen: implications for tumor immunotherapy. Cancer Immunol Immunother 2000;48:661–72.
13. Kyewski B, Derbinski J, Gotter J, Klein L. Promiscuous gene expression and central T-cell tolerance: more than meets the eye. Trends Immunol 2002;23:364–71.
14. Takase H, Yu CR, Mahdi RM, et al. Thymic expression of peripheral tissue antigens in humans: a remarkable variability among individuals. Int Immunol 2005;17:1131–40.
15. Engelhard VH, Bullock TN, Colella TA, Sheasley SL, Mullins DW. Antigens derived from melanocyte differentiation proteins: self-tolerance, autoimmunity, and use for cancer immunotherapy. Immunol Rev 2002;188:136–46.
16. Brichard V, Van Pel A, Wolfel T, et al. The tyrosinase gene codes for an antigen recognized by autologous cytolytic T lymphocytes on HLA-A2 melanomas. J Exp Med 1993;178:489–95.
17. Meek RL, Walsh KA, Palmiter RD. The signal sequence of ovalbumin is located near the NH2 terminus. J Biol Chem 1982;257:12245–51.
18. Camacho-Hubner A, Beermann F. Increased transgene expression by the mouse tyrosinase enhancer is restricted to neural crest-derived pigment cells. Genesis 2001;29:180–7.
19. Huard B, Arlettaz L, Ambrose C, et al. BAFF production by antigen-presenting cells provides T cell co-stimulation. Int Immunol 2004;16:467–75.
20. Schwaller J, Schneider P, Mhawech-Fauceglia P, et al. Neutrophil-derived APRIL concentrated in tumor lesions by proteoglycans correlates with human B-cell lymphoma aggressiveness. Blood 2007;109:331–8.
21. Huard B, Schneider P, Mauri D, Tschopp J, French LE. T cell costimulation by the TNF ligand BAFF. J Immunol 2001;167:6225–31.
22. Kalergis AM, Goyarts EC, Palmieri E, Honda S, Zhang W, Nathenson SG. A simplified procedure for the preparation of MHC/peptide tetramers: chemical biotinylation of an unpaired cysteine engineered at the C-terminus of MHC-I. J Immunol Methods 2000;234:61–70.
23. Maloy KJ, Erdmann I, Basch V, et al. Intralymphatic immunization enhances DNA vaccination. Proc Natl Acad Sci U S A 2001;98:3299–303.
24. Preynat-Seauve O, Schuler P, Contassot E, Beermann F, Huard B, French LE. Tumor-infiltrating dendritic cells are potent antigen-presenting cells able to activate T cells and mediate tumor rejection. J Immunol 2006;176:61–7.
25. Miller JF. Investigating a second thymus in mice. Science 2006;312:1597–8; author reply -8.
26. Denkberg G, Cohen CJ, Reiter Y. Critical role for CD8 in binding of MHC tetramers to TCR: CD8 antibodies block specific binding of human tumor-specific MHC-peptide tetramers to TCR. J Immunol 2001;167:270–6.
27. Allan RS, Smith CM, Belz GT, et al. Epidermal viral immunity induced by CD8α+ dendritic cells but not by Langerhans cells. Science 2003;301:1925–8.
28. Douillard P, Stoitzner P, Tripp CH, et al. Mouse lymphoid tissue contains distinct subsets of langerin/CD207 dendritic cells, only one of which represents epidermal-derived Langerhans cells. J Invest Dermatol 2005;125:983–94.
29. Nishimura EK, Jordan SA, Oshima H, et al. Dominant role of the niche in melanocyte stem-cell fate determination. Nature 2002;416:854–60.
30. Yajima I, Sato S, Kimura T, et al. An L1 element intronic insertion in the black-eyed white (Mitf[mi-bw]) gene: the loss of a single Mitf isoform responsible for the pigmentary defect and inner ear deafness. Hum Mol Genet 1999;8:1431–41.
31. Duttlinger R, Manova K, Chu TY, et al. W-sash affects positive and negative elements controlling c-kit expression: ectopic c-kit expression at sites of kit-ligand expression affects melanogenesis. Development 1993;118:705–17.
32. Kurts C, Kosaka H, Carbone FR, Miller JF, Heath WR. Class I-restricted cross-presentation of exogenous self-antigens leads to deletion of autoreactive CD8(+) T cells. J Exp Med 1997;186:239–45.
33. Morgan DJ, Kreuwel HT, Sherman LA. Antigen concentration and precursor frequency determine the rate of CD8+ T cell tolerance to peripherally expressed antigens. J Immunol 1999;163:723–7.
34. Lees JR, Charbonneau B, Swanson AK, et al. Deletion is neither sufficient nor necessary for the induction of peripheral tolerance in mature CD8+ T cells. Immunology 2006;117:248–61.
35. Mintern JD, Davey GM, Belz GT, Carbone FR, Heath WR. Cutting edge: precursor frequency affects the helper dependence of cytotoxic T cells. J Immunol 2002;168:977–80.
36. Lyman MA, Aung S, Biggs JA, Sherman LA. A spontaneously arising pancreatic tumor does not promote the differentiation of naive CD8+ T lymphocytes into effector CTL. J Immunol 2004;172:6558–67.
37. Lane C, Leitch J, Tan X, Hadjati J, Bramson JL, Wan Y. Vaccination-induced autoimmune vitiligo is a consequence of secondary trauma to the skin. Cancer Res 2004;64:1509–14.
38. Steitz J, Bruck J, Lenz J, Buchs S, Tuting T. Peripheral CD8+ T cell tolerance against melanocytic

self-antigens in the skin is regulated in two steps by CD4+ T cells and local inflammation: implications for the pathophysiology of vitiligo. J Invest Dermatol 2005; 124:144–50.
39. Lambe T, Leung JC, Bouriez-Jones T, et al. CD4 T Cell-Dependent Autoimmunity against a Melanocyte Neoantigen Induces Spontaneous Vitiligo and Depends upon Fas-Fas Ligand Interactions. J Immunol 2006;177: 3055–62.
40. Nichols LA, Chen Y, Colella TA, Bennett CL, Clausen BE, Engelhard VH. Deletional self-tolerance to a melanocyte/melanoma antigen derived from tyrosinase is mediated by a radio-resistant cell in peripheral and mesenteric lymph nodes. J Immunol 2007;179:993–1003.
41. Battyani Z, Xerri L, Hassoun J, Bonerandi JJ, Grob JJ. Tyrosinase gene expression in human tissues. Pigment Cell Res 1993;6:400–5.
42. Mancini L, Gubinelli M, Fortunato C, Carella R. Blue nevus of the lymph node capsule. Report of a case. Pathologica 1992;84:547–50.
43. Carson KF, Wen DR, Li PX, et al. Nodal nevi and cutaneous melanomas. Am J Surg Pathol 1996;20:834–40.
44. Hickman HD, Takeda K, Skon CN, et al. Direct priming of antiviral CD8+ T cells in the peripheral interfollicular region of lymph nodes. Nat Immunol 2008;9:155–65.
45. Kundig TM, Bachmann MF, DiPaolo C, et al. Fibroblasts as efficient antigen-presenting cells in lymphoid organs. Science 1995;268:1343–7.
46. Preynat-Seauve O, Contassot E, Schuler P, Piguet V, French LE, Huard B. Extralymphatic tumors prepare draining lymph nodes to invasion via a T-cell cross-tolerance process. Cancer Res 2007;67:5009–16.
47. Lee JW, Epardaud M, Sun J, et al. Peripheral antigen display by lymph node stroma promotes T cell tolerance to intestinal self. Nat Immunol 2007;8:181–90.
48. Rosenberg SA, Restifo NP, Yang JC, Morgan RA, Dudley ME. Adoptive cell transfer: a clinical path to effective cancer immunotherapy. Nat Rev Cancer 2008;8:299–308.
49. Overwijk WW, Theoret MR, Finkelstein SE, et al. Tumor regression and autoimmunity after reversal of a functionally tolerant state of self-reactive CD8+ T cells. J Exp Med 2003;198:569–80.